ChemComm
Chemical Communications

Accepted Manuscript

This article can be cited before page numbers have been issued, to do this please use: E. K. Kirkeby and A. Roberts, *Chem. Commun.*, 2020, DOI: 10.1039/D0CC03503C.

ROYAL SOCIETY OF CHEMISTRY

rsc.li/chemcomm

View Article Online
DOI: 10.1039/D0CC03503C

COMMUNICATION

Design, synthesis and characterization of structurally dynamic cyclic *N,S*-acetals

Received 00th January 20xx,
Accepted 00th January 20xx

DOI: 10.1039/x0xx00000x

Emily K. Kirkeby and Andrew G. Roberts*

We report the synthesis, characterization and comparison of a series of electronically perturbed, cyclic *N,S*-acetals. Inspired by electrophilic auxiliaries utilized for amine capture and concomitant peptide ligation, we studied these *N,S*-acetal systems and evaluated their propensity to generate zwitterionic intermediates *in situ*. Certain *N,S*-acetals in this study exhibit structurally dynamic properties through a solvent and pH-dependent ability to ring-open and ring-close via C1–S bond ionization at room temperature.

Chemical protein synthesis via peptide ligation methodologies is an enabling technology utilized for the advancement of biochemical discovery.[1] Native chemical ligation (NCL)[2] is the most frequently employed method to chemically join peptide sequences (**Fig. 1A**). This dependable ligation requires synthetic or semisynthetic access[3] to a *C*-terminal peptide thioester **1** and an *N*-terminal Cys peptide **2**. The reaction proceeds with a transthioesterification event, followed by an *S*-to-*N* acyl shift (*int*-**3**) to access ligated protein **3a** with an amide bond at Xaa–Cys, W = SH.[2,4] If desired, the Cys residue can be chemoselectively dethiylated, **3a**, W = SH → **3b**, W = H, providing Ala at the ligation site—a powerful advance referred to as *Ala ligation* (**Fig. 1A**).[5,6] A recent meta-analysis[7a] revealed that the two-step Ala ligation is used more frequently than NCL alone, due to the greater frequency of Ala (9% total abundance) compared with Cys residues (<2%) within proteins.[7] Naturally low Cys residue abundance has prompted the development of chemical methods for ligation at alternative sites, Xaa–Xaa, where Xaa is an '*acyl donor*' and Xaa is an '*acyl acceptor*'.[1,6]

Among the Cys-independent methodologies,[8] the development of aldehyde capture ligation (ACL) by Arora[9a] and Li[9b] represent a major advance toward the ideal of sequence-independent ligation (**4**, X = S or Se, **Fig. 1B**). The method leverages the chemoselective reactivity of an electrophilic *C*-terminal thioester-[9] or selenoester-[9b] benzaldehyde derivative (**4**, X = S or Se) and an amine partner (**5**) under aqueous conditions. First, a transiently generated hemiaminal *int*-**6'** undergoes *X*-to-*N* acyl shift, followed by the release of a peptide (**6**) with an amide bond at Xaa–Xaa.[9] ACL is a useful alternative for peptide ligation between sterically encumbered partners (*e.g.*, Val–Val), as well as for *C*-terminal partners considered to be epimerization prone (*e.g.*, Phe–Val). Although enabling, the electrophilic benzaldehyde component (**4**) must be

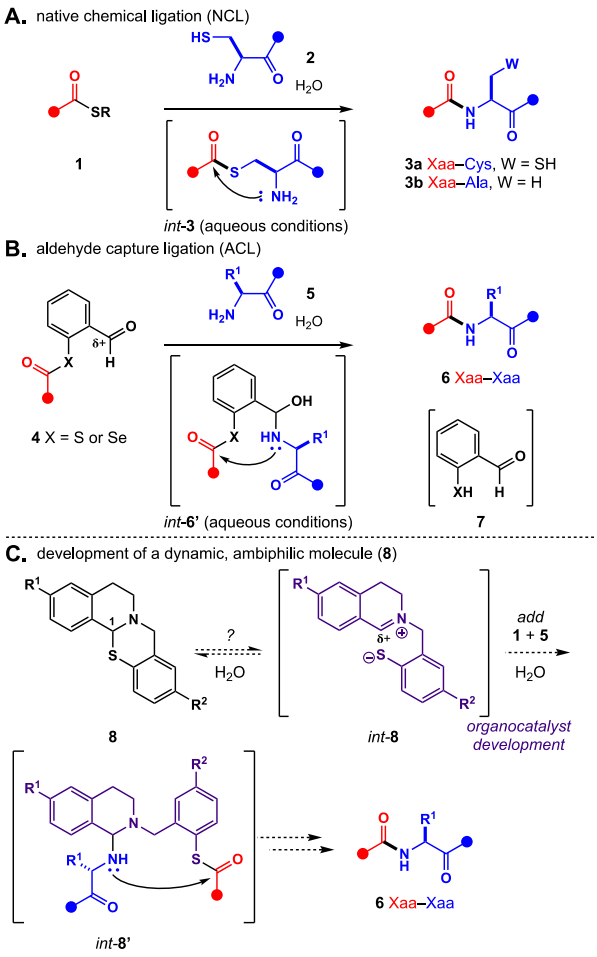

Figure 1 Native chemical ligation (A) and aldehyde capture ligation (B) inspire the design and characterization of a dynamic class of cyclic *N,S*-acetal molecules (C).

Department of Chemistry, University of Utah, 315 South 1400 East, Salt Lake City, Utah 84112, United States. e-mail: roberts@chem.utah.edu

†Electronic Supplementary Information (ESI) available: For ESI, including full procedures and characterization data, ^{1}H and ^{13}C NMR spectra, crystallographic data in CIF format (CCDC 2001038, 2001039, and 2001040) and computational information, see DOI: 10.1039/x0xx00000x

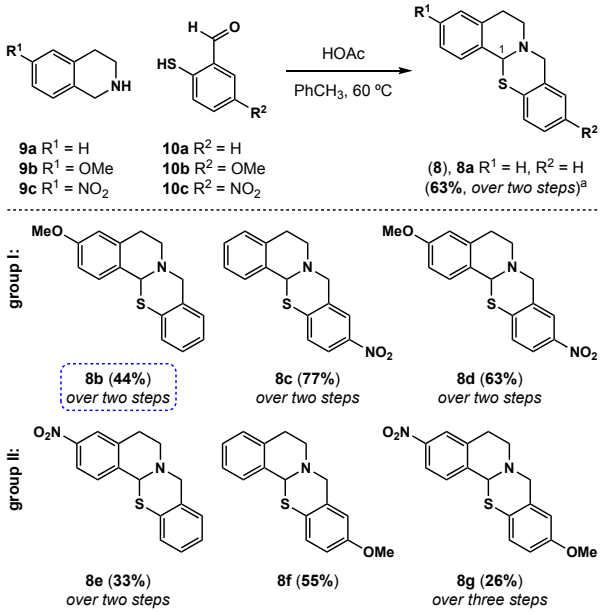

Scheme 1 Redox-neutral synthesis and study of seven *N*,*S*-acetal derivatives. [a]Yields are reported following multistep transformations that utilize crude 2-mercaptobenzaldehydes (**10a**-**10c**).

synthetically prepared and the stoichiometric auxiliary is ultimately discarded as **7** (X = S or Se) along with other unknown derivatives. These issues present the opportunity to design a dynamic, small molecule organocatalyst to facilitate concomitant transthioesterification and amine trapping reactions for procedurally improved sequence-independent peptide ligation (**Fig. 1C**).[8,9,10] Inspired by the productive reactivity of *N*,*O*-hemiaminal *int*-**6'**,[9a] we envisioned the study of a class of cyclic *N*,*S*-acetal molecules (**8**) designed with latent ambiphilicity. We hypothesize that a cyclic *N*,*S*-acetal (**8**) will exist in dynamic equilibrium with '*open*' form zwitterion *int*-**8**, revealing benzylic iminium (*electrophilic, δ+* at C1) and aryl thiolate functionalities.[11] An informed understanding of *int*-**8,** could facilitate the development of a general, organocatalyzed thioacyl aminolysis reaction, **1** + **5** → **6**, via proposed ternary adduct *int*-**8'**, under aqueous conditions.[9,10,12] We posited that controlled permutation and evaluation of electronics at positions R^1 and R^2 (**8**) would enable the discovery of a dynamic class of molecules. Through reactivity and spectroscopic characterization studies, we reveal the dynamic properties and reactivity exhibited by certain *N*,*S*-acetal variants (**8**).

In our study, we envisioned electronic perturbations that would affect ionization of the C1–S bond in *N*,*S*-acetal **8**.[11a] We designed a series of *N*,*S*-acetals (**8a**-**8g**) using Hammett substituent constants to predict ionization susceptibility *a priori* (Scheme 1).[13] In other words, we anticipate an *N*,*S*-acetal (**8**) with an electron donating substituent at R^1 (*e.g.*, R^1 = OMe) and/or an electron withdrawing substituent at R^2 (*e.g.*, R^2 = NO_2) to favor C1–S bond ionization relative to either converse case. The comparative study and characterization of *N*,*S*-acetals organized into two groups, group I: **8b**, **8c**, **8d**, and, group II: **8e**, **8f**, **8g**, relative to the parent null, **8a**, might offer further insight. Accordingly, designed *N*,*S*-acetals were synthesized using the redox-neutral sulfenylation chemistry described by Seidel and co-workers.[11a] This acid-promoted reaction combines commercially available 1,2,3,4-tetrahydroisoquinolines (**9a**-**9c**) reacted with prepared 2-mercaptobenzaldehydes (**10a**-**10c**) (*see the* ESI†). All seven *N*,*S*-acetal variants **8a**-**8g** were purified by trituration with ethyl acetate and isolated as solids in useful yields, with derivatives **8d**-**8g** being previously unknown. Preliminary studies using ^{1}H NMR spectroscopy (500 MHz, $CDCl_3$) to characterize **8b**, **8c**, and **8d** were perplexing. We observed spectral line broadening in the upfield region (δ ppm, 4.75-2.25), while the downfield regions (δ ppm, 10.0-5.5) were resolved as one would expect. Despite being previously characterized,[11a] the spectroscopic anomalies in comparative ^{1}H NMR spectra for **8a** and **8b** were not explained. Overall, the phenomenal spectral features observed for **8b**, **8c**, and **8d** were seemingly incongruent with comparative data for **8a**, **8e**, **8f**, and **8g**. However, the general observations based on data appeared to be naturally in line with our initial hypotheses concerning C1–S ionization susceptibility. Further investigation revealed an intriguing dynamic behavior exhibited by the study of **8b**, **8c** and **8d** in solvents of varied polarity.

A comparative analysis of ^{1}H NMR spectra (500 MHz, $CDCl_3$, δ ppm, 4.75-2.25) for **8a**-*top* and **8b**-*middle* (**Fig. 2**) serves to emphasize the impact that a single methoxy group exhibits on the *N*,*S*-acetal system. Null system **8a** exhibits complete resolution for each diastereotopic methylene proton: H^b (4.56, d, *J* = 16.6 Hz, 1H), $H^{b'}$ (3.96, d, *J* = 16.6 Hz, 1H), $H^{cc'}$ (3.22, m, 2H), $H^{dd'}$ (2.86, m, 2H). The respective methylene protons, $H^{bb'}$, $H^{cc'}$, and $H^{dd'}$, in the methoxy variant (**8b**) exhibit significant line broadening, despite total resolution of the methoxy group, CH_3O- (3.79, s, 3H), and the downfield region (δ (ppm), 10.0-5.5). Intriguingly, this odd behavior is subject to changes in solvent polarity (*see* ESI† **Fig. S-2**, **Fig. S-3**). Analysis of the ^{1}H NMR spectrum of **8b** in benzene-d_6 (500 MHz, C_6D_6) exhibits total resolution (**Fig. 2**, *bottom*), including for respective

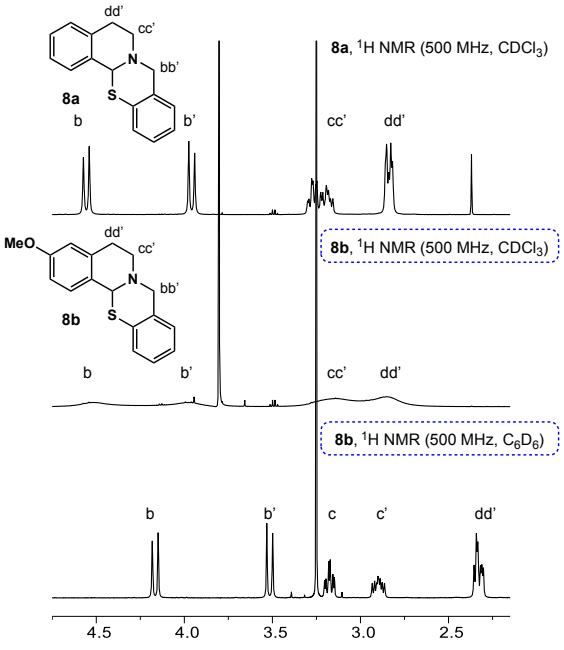

Figure 2 Characterization of *N*,*S*-acetals (**8a**, **8b**) by ^{1}H NMR spectroscopy.

methylene protons: H^b (4.21, d, *J* = 16.6 Hz, 1H), $H^{b'}$ (3.56, d, *J* = 16.6 Hz, 1H), CH_3O- (3.29, s, 3H), H^c (3.22, td, *J* = 11.8, 4.3 Hz, 1H), $H^{c'}$ (2.94, ddd, *J* = 18.2, 12.0, 6.6 Hz, 1H), $H^{dd'}$ (2.37, m, 2H).

Intriguingly, select variants **8b**, **8c** and **8d** (group I) in the series exhibit dynamic properties observable by ^{1}H NMR spectroscopy (*see* ESI†).[11,14] In the exemplary case of methoxy-substituted variant, **8b**, we observe significant ^{1}H signal broadening for methylene positions $H^{bb'}$, $H^{cc'}$ and $H^{dd'}$ in $CDCl_3$ at ambient conditions. Contrarily, the entire ^{1}H spectrum is resolved in benzene-d_6. This solvent-controlled dynamicity is also temperature dependent. For example, the characterization of **8b** by variable temperature ^{1}H NMR demonstrates that cooling from 21 °C (broadened signals) to –45 °C in $CDCl_3$ results in spectral resolution (**Fig. 3A,** *see* ESI† **Fig. S-1**).

We attribute these observations to a dynamic equilibrium of interconverting *antiperiplanar* and *synperiplanar* diastereoisomers (**Fig. 3B**). The respective nomenclatures describe the relationship between the lone pair at nitrogen and the C1–S bond. The depicted *antiperiplanar* conformer (**8b**-*antiperiplanar*, *shown*) is presumed to be thermodynamically favored, the nitrogen lone pair is oriented anti to the C1–S bond, this is also confirmed by x-ray crystallography (**Fig. 3B**, for x-ray structures of **8a** and **8d**, *see* ESI†). This type of stereospecific dynamicity has been previously described for alkaloid *N*,*O*-acetal systems and highlights the importance of stereochemistry at nitrogen.[15] In the parent null case, **8a** (R^1 = H, R^2 = H), and for group II variants (**8e**, **8f**, and **8g**) interconversion from *antiperiplanar* to *synperiplanar* form at room temperature is presumed to be disfavored. These *N*,*S*-acetals, **8a**, **8e**, **8f** and **8g**, exhibit fully resolved ^{1}H NMR spectra in both $CDCl_3$ and benzene-d_6. However, in the methoxy substituted case **8b** (*shown*), this interconversion is proposed to be facile and this room temperature equilibration is responsible for the signal broadening observed in $CDCl_3$. Benzene-d_6 is hypothesized to destabilize the zwitterionic *int*-**8b**, precluding the interconversion of the *antiperiplanar* and *synperiplanar* diastereoisomers. These observations distinguish the chemical dynamicity of group I *N*,*S*-acetals (**8b**, **8c**, **8d**) and the importance of electronic perturbations to their reactivity.

Using theory-based computation to study mechanism, Houk, Seidel and coworkers previously suggested *int*-**8a** to be the penultimate intermediate *en route* to the formation of **8a** from the reaction of **9a** with **10a** (**Scheme 1**).[11a] Accordingly, relative energy values obtained from quantum mechanical modelling[11] of *N*,*S*-acetals, **8a**, **8d**, **8g**, and their respective zwitterionic forms, *int*-**8a** (R^1 = H, R^2 = H), *int*-**8d** (R^1 = OMe, R^2 = NO_2) and *int*-**8g** (R^1 = NO_2, R^2 = OMe), support a C1–S bond ionization susceptibility rank of: **8d** > **8a** > **8g** (*see* ESI† **Fig. S-7**). This relative comparison of the extremely polarized cases, **8d** and **8g**, is consistent with our qualitative spectroscopic observations. A solution of *N*,*S*-acetal **8d** in $CDCl_3$ at room temperature is structurally dynamic, whereas variant **8g** is not.

To further understand this solvent-dependent dynamic behavior, we reasoned that a zwitterionic intermediate *int*-**8** may be directly observable spectroscopically or inferred by trapping either the benzylic iminium or thiolate functionalities to form a stable derivative. Thus, we developed an

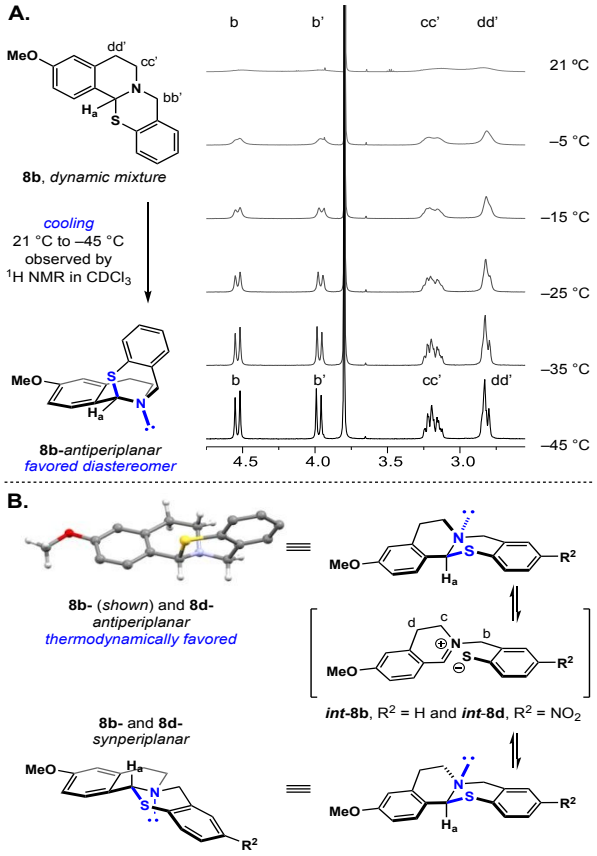

Figure 3 (A) Variable temperature ^{1}H NMR spectroscopy in $CDCl_3$, 21 °C to –45 °C, demonstrates **8b**-*antiperiplanar* as the favored diastereomer; (B) Proposed equilibration of two diastereoisomeric forms: Impact of electronics and stereoelectronics on structural dynamics (**8b** and **8d**).

understanding of dynamic reactivity for group I *N*,*S*-acetals, **8b**, **8c** and **8d**, under more extreme conditions (**Scheme 2**). The reaction of **8b** [16 mM] under acidic conditions, **a.** *neat* CF_3CO_2H, or **b.** 10 *equiv* CF_3CO_2H in $CDCl_3$, forms the protonated form of *int*-**8b** rapidly, *<1 min for condition* ***b***, and quantitatively (> 95% purity ^{1}H NMR). This benzylic iminium *int*-**8b** is characterized by ^{1}H, ^{13}C and 2-D NMR experiments (*see* ESI† **Fig. S-4**, **Fig. S-5**, **Fig. S-6**). Notably, the methine H^a and C1 signals are diagnostic (500 MHz, $CDCl_3$), as signals shift from *N*,*S*-acetal **8b** (H^a = 6.14 ppm, C1 = 67.1 ppm) to benzylic iminium *int*-**8b** (H^a = 8.57 ppm, C1 = 163.9 ppm). As expected, methylene signals, H^b, H^c and H^d, for *int*-**8b** are homotopic and fully resolved. Similar ring-opening results are observed for the additional group I *N*,*S*-acetal variants, **8c** and **8d** (*see* ESI†).

This *N*,*S*-acetal (**8b**) ionization process is reversible (**Scheme 2**). Titration of crude *int*-**8b** from $CDCl_3$ experiment (*condition* ***b***) with 10 *equiv* triethylamine (*condition* ***c***) quantitatively reforms the '*closed*' form, *N*,*S*-acetal **8b**, as observed by ^{1}H NMR spectroscopy (*see* ESI† **Fig. S-4**). Interestingly, reclosure is also affected by altering the polarity of the solvent mixture.

Treatment of crude *int*-**8b** from $CDCl_3$ experiment (*condition* ***b***) with 100 *equiv* CH_3OH (*condition* ***d***) reforms *N,S*-acetal **8b** as observed by thin-layer chromatography and ^1H NMR

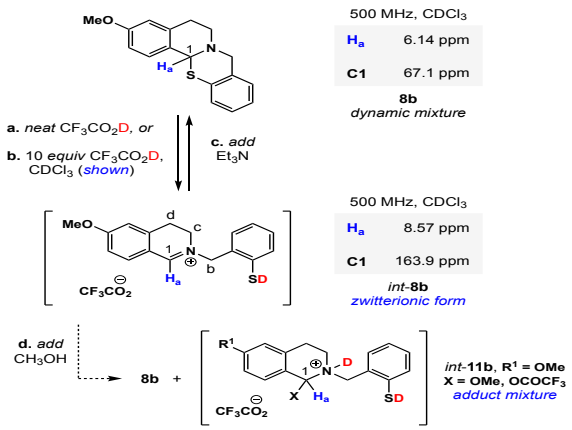

Scheme 2 *N,S*-acetal **8b**, C1–S ionization, chemically induced formation of zwitterion *int*-**8b** and reactivity.

spectroscopy. Anticipated *in situ* formed adducts consistent with *N,O*-acetals (**11b**, X = OMe or $OCOCF_3$) are not detected.[16]

Further studies will evaluate the propensity of benzylic iminium *int*-**8b** to undergo addition-type reactions with various nucleophiles, including amines, alcohols and thiols.[16,17] Collectively, these results suggest that the development of pH controlled, buffered conditions may permit systematic *N,S*-acetal opening and closure reactivity. Further studies will involve the generation and reactivity characterization of *N,S*-acetal derived scaffold–peptide adducts (*e.g.*, *int*-**8'**, **Fig. 1C**) toward the development of an organocatalysis platform for sequence-independent peptide ligation.[18] The understanding of group I *N,S*-acetal (**8b**, **8c**, **8d**) reactivity may also have implications for the control of nucleophile capture and release events important to *X,S*-acetal systems (X = O or N)[19] and dynamic covalent chemistry derived materials.[20]

We are grateful for financial support from the University of Utah. Computational resources were provided by the Center for High Performance Computing at the University of Utah. We thank Lori D. Digal for helpful discussions. We also thank Samantha Grosslight and Dr. Jolene P. Reid (Sigman Laboratory) for assistance with computations, Dr. Ryan VanderLinden for x-ray crystallographic analyses and Dr. Peter Flynn of the University of Utah for assistance with variable temperature NMR experiments. NMR results included in this report were recorded at the David M. Grant NMR Center, a University of Utah Core Facility. Funds for construction of this center and the helium recovery system were obtained from the University of Utah and the National Institutes of Health (NIH) awards 1C06RR017539-01A1 and 3R01GM063540-17W1, respectively. NMR instruments were purchased with support of the University of Utah and the NIH award 1S10OD25241-01.

Conflicts of interest

There are no conflicts to declare.

Notes and references

View Article Online
DOI: 10.1039/D0CC03503C

‡ CCDC 2001038 (**8a**), 2001039 (**8b**) and 2001040 (**8d**) contain the supplementary crystallographic data for this paper. The data can be obtained free of charge from The Cambridge Crystallographic Data Centre via www.ccdc.cam.ac.uk/getstructures.

1 (a) S. B. H. Kent, *J. Pept. Sci.*, 2015, **21**, 136–138; (b) S. Kent, Bioorg. Med. Chem. 2017, **25**, 4926–4937.
2 P. E. Dawson, T. W. Muir, I. Clark-Lewis and S. B. Kent, *Science* 1994, **266**, 776–779; (b) T. M. Hackeng, J. H. Griffin and P. E. Dawson, P. E., *Proc. Natl. Acad. Sci.* USA 1999, **96**, 10068–10073.
3 T. W. Muir, D. Sondhi and P. A. Cole, *Proc. Natl. Acad. Sci. USA*, 1998, **95**, 6705–6710.
4 E. C. B. Johnson and S. B. Kent, *J. Am. Chem. Soc.*, 2006, **128**, 6640–6646.
5 (a) L. Z. Yan, and P. E. Dawson, *J. Am. Chem. Soc.*, 2001, **123**, 526–533; (b) Q. Wan, and S. J. Danishefsky, *Angew. Chem. Int. Ed.*, 2007, **46**, 9248–9252.
6 (a) H. M. Burke, L. McSweeney and E. M. Scanlan, *Nature Comm.*, 2017, **8**, 15655. (b) S. Kulkarni, J. Sayers, B. Premdjee and R. J. Payne, *Nature Rev. Chem.*, 2018, ***2***, 0122.
7 (a) V. Agouridasa, O. E. Mahdib, M. Cargoëta and O. Melnyk, *Bioorg. Med. Chem.* 2017, **25**, 4938–4945; (b) M. T. Jacobsen, P. W. Erickson, M. S. Kay, *Bioorg Med Chem.* 2017, **25**, 4946–4952.
8 (a) Y. Chow and X. Li, *Tetrahedron Lett.*, 2015, **56**, 3715–3720; (b) J. Yang, J. Zhao, *J. Sci. China Chem.* 2018, **61**, 97–112.
9 (a) M. Raj, H. Wu, S. L. Blosser, M. A. Vittoria and P. S. Arora, *J. Am. Chem. Soc.*, 2015, **127**, 6932–6940; (b) C. L. Tung, C. T. T. Wongab and X. Li, *Org. Biomol. Chem.*, 2015, **13**, 6922–6926.
10 For selected related approaches, see: (a) S. Leleu, M. Penhoat, A. Bouet, G. Dupas, C. Papamicaël, F. Marsais and V. Levacher, V. *J. Am. Chem. Soc.*, 2005, **127**, 15668–15669; (b) H. Wu, Handoko, M. Raj and P. S. Arora, *Org. Lett.*, 2017, **19**, 5122–5125; (c) Handoko, S. Satishkumar, N. R. Panigrahi and P. S. Arora, *J. Am. Chem. Soc.*, 2019, **141**, 15977–15985.
11 (a) C. L. Jarvis, M. T. Richers, M. Breugst, K. N. Houk and D. Seidel, *Org. Lett.* 2014, **16**, 3556–3559; (b) M. T. Richers, M. Breugst, A. Yu, A. Y. Platonova, A. Ullrich, A. Dieckmann, K. N. Houk and D. Seidel, *J. Am. Chem. Soc.* 2014, **136**, 6123–6135.
12 At appropriate concentrations, unhindered thioacyl aminolysis ligations can proceed uncatalyzed. Intramolecular thioacyl aminolysis reactions can also be efficient, see: (a) R. J. Payne, S. Ficht, W. A. Greenberg and C.-H. Wong, *Angew. Chem. Int. Ed.*, 2008, **47**, 4411–4415; (b) Y. Li, A. Yongye, M. Giulianotti, K. Martinez-Mayorga, Y. Yu and R. A. Houghten, *J. Comb Chem.*, 2009, **11**, 1066–1072.
13 C. Hansch, A. Leo, R. W. Taft, *Chem. Rev.*, 1991, **91**, 165–195. (σ_{para}: H– = 0, MeO– = -0.27, O_2N– = 0.78)
14 R. G. Bryant, *J. Chem. Educ.*, 1983, **60**, 933.
15 B. Herberich, J. D. Scott and R. M. Williams, *Bioorg. Med. Chem.* 2000, **8**, 523–532.
16 J. Dhineshkumar, M. Lamani, K. Alagiri, and K. R. A. Prabhu, *Org. Lett.*, 2013, **15**, 1092–1095.
17 For a representative method, see: T. Suga, S. Iizuka and T. Akiyama, *Org. Chem. Front.* 2016, **3**, 1259.
18 Preliminary studies support the dynamic reactivity of *N,S*-acetals with amino acids. For example, an aqueous solution of **8a** (1 *equiv*) and H-Gly-OH (2 *equiv*) generates a tentatively assigned Gly-adduct ***int*-11a** (Scheme 2, X = Gly-OH, R^1 = H) as observed by UPLC-MS ($[M+Gly-OH+H]^+$: 329.13; obsd: 329.30)
19 For a representative example, see: L. R. Malins, J. N. deGruyter, K. J. Robbins, P. M. Scola, M. D. Eastgate, M. R. Ghadiri, P. S. Baran, *J. Am. Chem. Soc.*, 2017, **139**, 5233–5241.
20 Y. Zhang and O. Ramström, *Chem. Eur. J.*, 2014, **20**, 3288–3291.

View Article Online
DOI: 10.1039/D0CC03503C